International
Progress Report

IPR-04-30

Äspö Hard Rock Laboratory

Äspö Task Force

Task 6A, 6B and 6B2

Modelling of sorbing tracer breakthrough for Tasks 6A, 6B and 6B2

Hua Cheng
Vladimir Cvetkovic

Water Resources Eng., KTH

April 2003

Svensk Kärnbränslehantering AB
Swedish Nuclear Fuel
and Waste Management Co
Box 5864
SE-102 40 Stockholm Sweden
Tel 08-459 84 00
+46 8 459 84 00
Fax 08-661 57 19
+46 8 661 57 19

Äspö Hard Rock
Laboratory

Report no.
IPR-04-30
No.
F65K
Author
Hua Cheng
Vladimir Cvetkovic
Date
April 2003
Checked by
Jan-Olof Selroos
Date
July 2004
Approved
Christer Svemar
Date
2004-08-30

Äspö Hard Rock Laboratory

Äspö Task Force

Task 6A, 6B and 6B2

Modelling of sorbing tracer breakthrough for Tasks 6A, 6B and 6B2

Hua Cheng
Vladimir Cvetkovic

Water Resources Eng., KTH

April 2003

Keywords: Single fractures, transport, retention, modelling, crystalline rock, Task 6, Äspö Task Force

Abstract

This report presents the modelling results for Tasks 6A, 6B and 6B2 by the WRE/KTH team using the LaSAR framework.

The modelling results of Task 6A re-examine the STT-1B sorbing tracer test results. The modelled breakthrough curves (BTCs) for both the experimental injection and Dirac pulse injection are provided. The breakthrough times at 5%, 50% and 95% mass recovery are also provided.

Task 6B is modelled on the same flow path as for Task 6A while with a flow rate 1000 times lower in order to match the performance assessment (PA) time scale. The modelled BTCs for a constant injection of 1 MBq/y and for Dirac pulse injection are provided. The breakthrough times at 5%, 50% and 95% mass recovery for Dirac pulse injection are presented as well.

In Task 6B2 the flow is assumed to occur in a two-dimensional fracture flow configuration. The tracers are injected along a 2-meter line source. The tracers are assumed to be collected at a line 10 meters downstream. The flow in the planar fracture is driven by a hydraulic gradient of 0.1% between two intersecting fractures. The modelled BTCs for a constant injection of 1 MBq/y and for Dirac pulse injection are provided as well as the breakthrough times at 5%, 50% and 95% mass recovery for Dirac pulse injection.

Results show that for Dirac injection, the ratios between the respective mass recovery times for the two bounding porosity values are always larger than the ratio of the porosity itself (which is 2). The results of Tasks 6B and 6B2 show that the parameter β has a strong influence on the retention and transport of the tracers, and therefore on the breakthrough curves of the tracers.

Sammanfattning

Denna rapport presenterar resultat för modelleringsuppgifterna Task 6A, 6B och 6B2. Resultaten är framtagna av modelleringsgruppen WRE/KTH som har använt konceptet LaSAR.

Modelleringsresultaten för Task 6A belyser på nytt resultaten från spårförsöket STT-1B med sorberande ämnen. Både modellerade genombrottskurvor för själva experimentet och för en Diracpulsinjektion redovisas. Genombrottstider för 5%, 50% och 95% redovisas.

Modelluppgift Task 6B är modellerad för samma flödesväg som i fallet Task 6A, men med ett flöde som är 1000 gånger mindre för att stämma överens med framtida förvarsförhållanden. Modellerade genombrottskurvor för en konstant injektion av 1 MBq/år och för en Diracpuls presenteras. Genombrottstider för 5%, 50% och 95% redovisas även i detta fall.

I Task 6B2 antas flödet ske i en tvådimensionell flödeskonfiguration. Spårämnena injiceras utmed en två meter lång linjekälla. Spårämnena samlas upp utmed en linje 10 m nedströms. Flödet i den plana sprickan drivs av en hydraulisk gradient på 0,1% mellan två korsande sprickor. Modellerade genombrottskurvor för en konstant injektion av 1 MBq/år och för en Diracpuls presenteras. Dessutom redovisas genombrottstider för 5%, 50% och 95% av injicerad mängd av Diracpulsen.

Resultaten visar att för Diracpulsinjiceringen är kvoten mellan respektive tider för mängd återerhållen massa alltid större än själva porositetskvoten som har värdet 2. Resultaten för Task 6B och 6B2 visar att parametern β har en stark påverkan på fördröjningen och transporten av spårämnen och därför på genombrottskurvorna för dessa spårämnen.

Executive summary

Objectives

Task 6 of the Task Force on Groundwater Flow and Solute Transport is aimed at bridging between site characterisation (SC) and performance assessment (PA) approaches to solute transport and retention in fractured rocks. In the first three subtasks, Tasks 6A, 6B and 6B2, fluid flow and solute transport in a detailed spatial scale 5-10 m within a single fracture in Feature A (Winberg et al., 2000) are modelled. The modelling results of the first three subtasks are provided in this report.

In Task 6A the results of the STT-1B sorbing tracer test in the first stage of the TRUE program, TRUE-1 (Andersson et al., 1999) are re-modelled and the task provides a basis for the subsequent modelling tasks. Task 6B aims at modelling flow and transport in a PA time scale on the same flow path used in Task 6A. Task 6B2 also aims at modelling flow and transport in a PA time scale, but in a two-dimensional flow configuration with a line source of injection instead of injecting and pumping tracers through boreholes.

Modelling Tasks

Task 6A is modelled on the same flow path as in the STT-1B test in TRUE-1, i.e., the path between the injection borehole KXTT1 and the pumping borehole KXTT3, and using the same pumping flow rate 400 mL/min as for STT-1B.

Task 6B is modelled on the same flow path as in Task 6A, but with a 1000 times lower flow rate in order to match the PA time scale.

Task 6B2 is modelled with a uniform flow configuration in a planar fracture. The tracers in Task 6B2 are injected along a line source two meters in length. The flow is driven by a hydraulic gradient of 0.1% between two intersecting fractures. The tracers are collected 10 meters downstream.

Model description

The Lagrangian Stochastic Advection and Retention (LaSAR) approach (Cvetkovic et al., 1999, 2000) is used in the modelling. Feature A is assumed to be a planar fracture with variable spatial apertures. The distribution of the apertures is approximated to be lognormal with an exponential correlation structure. The porosity is assumed to be constant.

The following mass transfer processes are accounted for in the modelling: advection, dispersion, sorption on fracture surface, and diffusion/sorption in the rock matrix.

A linear τ-β relationship inferred from the TRUE-1 evaluation (Cvetkovic et al., 2000) is used in calculating the breakthrough curves (BTCs) in Tasks 6A and 6B. The distribution of τ is assumed to be inverse-Gaussion. The moments of τ calibrated in the TRUE-1 evaluation for STT-1B are also used in Tasks 6A and 6B.

Monte-Carlo simulations are performed for Task 6B2 in order to obtain τ and β distributions. The obtained τ and β distributions are used directly in calculating the BTCs in Task 6B2.

In the modelling for Tasks 6A, 6B and 6B2, the best estimates of sorption and diffusion parameters from the TRUE-1 evaluation are used. In Task 6B, a second set of modelling results are also provided using an additional porosity of a lower value. Since for Task 6B the flow and transport is modelled on a PA time scale, the tracers have much longer time to diffuse more deeply into the rock matrix where the porosity is lower than in the rim zone adjacent to the fracture surface. That gives the reason to use a lower value of porosity. The mean of the residence time τ in Task 6B is obtained as 1000 times that in Task 6A, since the flow rate is 1000 times lower. The variance of τ is calculated so that the coefficient of variation is the same as in Task 6A.

In Task 6B2, a second set of modelling results are also provided using a porosity of MIDS value (modelling input data set) (Byegård et al., 1998). The simulated τ, β data from Monte-Carlo simulations are used directly in the calculation of BTCs in Task 6B2.

Results

The BTCs for all tracers studied are provided for both experimental injection and Dirac pulse injection for Task 6A. The times of 5%, 50% and 95% mass recovery and the maximum release rates are also provided for both injections for Task 6A.

In Task 6B, the BTCs for a constant injection of 1 MBq/y and for Dirac pulse injection are provided. The times of 5%, 50% and 95% mass recovery and the maximum release rates are also provided for Dirac pulse injections for Task 6B.

The BTCs for a constant injection of 1 MBq/y and for Dirac pulse injections are provided for Task 6B2. The times of 5%, 50% and 95% mass recovery and the maximum release rates are also provided for Dirac pulse injections for Task 6B2.

Discussions

There are differences between the BTCs of the same tracer in Tasks 6B and 6B2, when using the same porosity and the same value of sorption coefficient. The retention of the tracer is stronger in Task 6B2 than in Task 6B. The reason for the difference is that, in Task 6B2, the values of β are obtained from Monte-Carlo simulations while in Task 6B, the values of β are assumed to be linearly related to the water residence time τ. It turns out that the values of β are a few times larger in Task 6B2 than in Task 6B. The retention is determined by two parameter groups of products $\beta\kappa$ and βK_a, where κ depends on the porosity, diffusivity and sorption coefficient of the tracers. Even though κ is smaller in Task 6B2, the overall product of the two parameters $\beta\kappa$ is larger for Task 6B2 than for Task 6B. This is also true for the product βK_a.

Contents

List of tables

List of figures

1 Introduction

To improve the confidence in radionuclide transport modelling for the Swedish bedrock, SKB has initiated a tracer test program referred to as Tracer Retention Understanding Experiments (TRUE). In the TRUE program, breakthrough curves (BTCs) for both conservative and sorbing tracers obtained in field experiments in the Äspö Hardrock Laboratory are compared with different modelling results. The TRUE program has been divided into different stages: stages in detailed scale (<10 m) and in block scale (10 – 50 m). To bridge between site characterisation (SC) and performance assessment (PA) approaches to solute transport and retention in fractured rocks, Task 6 within the Äspö Task Force was established. In Task 6, these two types of modelling approaches will be applied for the experimental boundary conditions and the PA scale boundary conditions.

The first three sub-tasks within Task 6 are: Task 6A (Selroos and Elert, 2001), 6B (Selroos and Elert, 2001), and 6B2 (Elert and Selroos, 2001), which aim at testing the two types of modelling approaches in a detailed spatial scale (5 - 10 m).

The purpose of Task 6A is to re-model the STT-1B sorbing tracer test results (Andersson et al., 1999) in the detailed scale stage of the TRUE program, i.e., TRUE-1 (Winberg et al., 2000). The modelling of Task 6A is performed on the same test configuration as in the STT-1B test, i.e., with a radially converging flow and transport between the injection borehole (KXTT1) and the pumping borehole (KXTT3), and with a pumping rate of 400 mL/min (Figure 1-1).

The modelling of Task 6B is carried out on the same flow path as in Task 6A, but in a PA time scale. This is achieved with a much lower flow rate compared to that in Task 6A, hence a much longer residence time.

Task 6B2 is performed on a uniform flow configuration where the flow and transport occur in a much larger area of Feature A. The injection and the pumping will not be carried out in a single borehole, but in a section of a fracture. The flow is driven by a hydraulic gradient between two parallel fractures intersecting Feature A.

This report presents the modelling results of Tasks 6A, 6B and 6B2 by the WRE/KTH team using the LaSAR approach (Cvetkovic et al., 1999, 2000).

For all three subtasks, the modelled breakthrough curves, the times for 5%, 50% and 95% mass recovery of the tracers, and the maximum release rates will be provided.

2 Modelling Tasks

In all of the three subtasks, i.e., Tasks 6A, 6B and 6B2, the breakthrough curves (BTCs) of the following tracers are modelled: iodine (I-131), strontium (Sr-85), cobalt (Co-58), technetium (Tc-99m) and americium (Am-241).

2.1 Task 6A

Task 6A is performed in the same test configuration as in the STT-1B test, i.e., with a radially converging flow between two boreholes KXTT1 R2 and KXTT3 R2 in Feature A of the STT-1b test (Figure 2-1) with a pumping rate of 400 mL/min. The injection histories of I-131, Sr-85, Co-58 from STT-1B are used. The injection histories of technetium and americium are assumed to be identical to those of cobalt in the STT-1B test. The modelling results of the tracer BTCs for Dirac pulse input will also be provided.

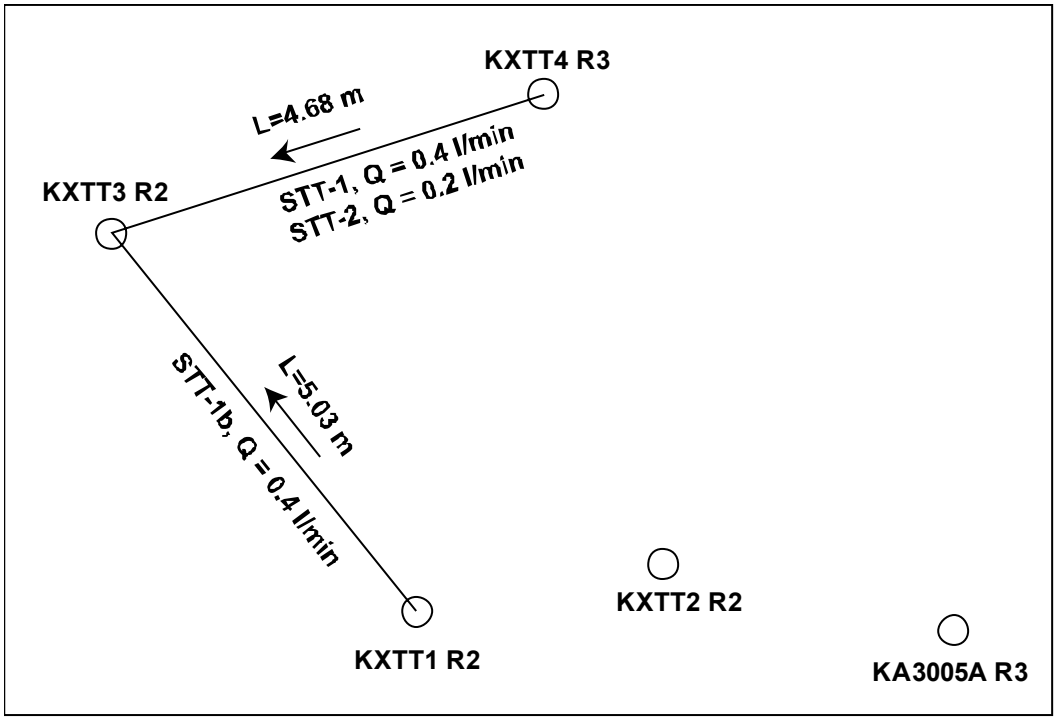

Figure 2-1. *Test configuration for the sorbing tracer tests STT-1, STT-1b and STT-2. Q is the pumping rate. L is the distance between injection and pumping boreholes (from Task 6A and 6B modeling task specification).*

2.2 Task 6B

In Task 6B, the breakthrough curves (BTCs) of the tracers are modelled for both constant injection of 1MBq/y and Dirac pulse input on the same path as in Task 6A (Figure 2-1). The flow rate, however, is 1000 times lower than that of Task 6A in order to match the PA time scale.

2.3 Task 6B2

In Task 6B2, the flow and transport are assumed to occur in a fracture with uniform flow configuration in Feature A. The tracers are injected along a 2-meter line source. The recovery of the tracers is performed in a fracture-intersecting Feature A and is 10 meters downstream (Figure 2-2). The flow is driven by a hydraulic gradient of 0.1% between the two fractures that intersect Feature A. In contrast, the flow in Tasks 6A and 6B is caused by pumping through a borehole.

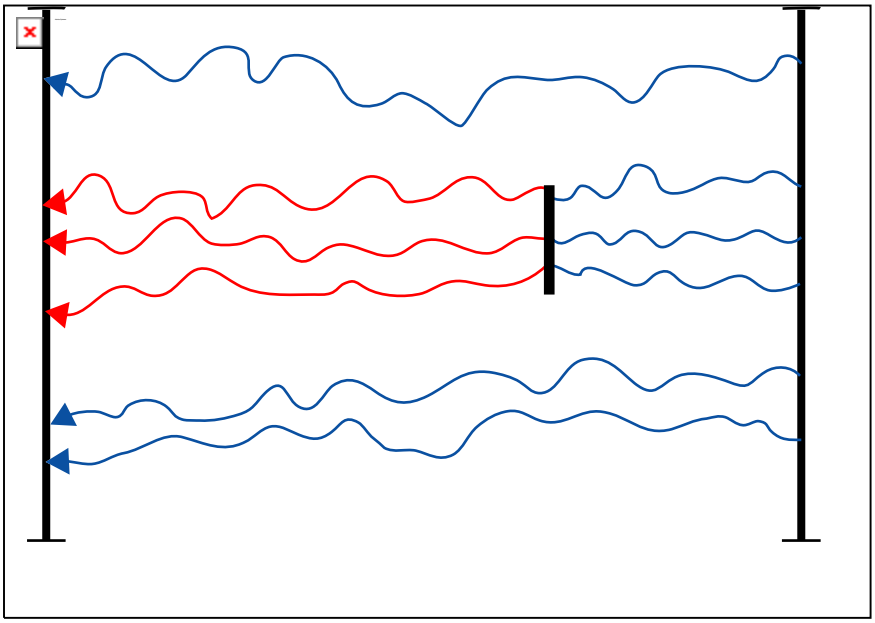

Figure 2-2. *Test configuration for Task 6B2 (from Task 6B2 modelling task specification).*

3 Model description

The Lagrangian Stochastic Advective Reaction (LaSAR) framework is presented in Cvetkovic et al., 1999. The framework was applied for prediction and evaluation modelling in the first stage of TRUE tracer tests (Cvetkovic et al., 2000). The framework was extended from a single heterogeneous fracture to a network of heterogeneous fractures and applied for modelling TRUE Block Scale tracer tests (Cvetkovic and Cheng, 2002). The LaSAR approach is employed in the Task 6D modelling in this report.

3.1 Geometrical description

Feature A is conceptualised as a single planar heterogeneous fracture with variable spatial aperture. The distribution of the aperture is approximated to be lognormal with an exponential correlation structure. The porosity is assumed to be constant.

3.2 Processes considered

As a tracer is injected into the fracture, it will be advected and dispersed. The tracer may also be subject to mass transfer processes. In the modelling, the following mass transfer processes are considered: sorption on the fracture surface, diffusion into the rock matrix and sorption on the inner surface of the rock matrix. The following assumptions are made concerning the transport:

- All mass transfer processes are linear.
- The relationship between the water residence time τ and the parameter β (Cvetkovic et al., 1999; 2000) is assumed to be linear (for Tasks 6A and 6B).
- The tracers are transported into the rock matrix only by diffusion, i.e., there is no advective transport in the rock matrix. The diffusion into the rock matrix is one-dimensional (the diffusive flux is perpendicular to the fracture plane).
- The dispersion in the fracture is longitudinal only (parallel to the fracture plane).

With these processes considered, the solution along a streamline for a pulse injection is (Cvetkovic et al., 2000)

$$\gamma(t,\tau;\beta) = \frac{H(t-\tau-\beta K_a)\beta\kappa}{2\sqrt{\pi}(t-\tau-\beta K_a)^{3/2}} \exp\left[\frac{-\beta^2\kappa^2}{4(t-\tau-\beta K_a)}\right] \qquad (3\text{-}1)$$

where $\kappa = \theta\sqrt{D(1+K_d^m)}$

Taking into account the dispersion effect and assuming the joint distribution of τ and β is $g(\tau, \beta)$, the tracer breakthrough can be calculated by

$$q(x,t) = \int_0^\infty \int_0^\infty \gamma(t;\tau,\beta) g(\tau,\beta;x) d\tau d\beta \qquad (3\text{-}2)$$

For a continuous injection ϕ(t), the breakthrough is obtained by

$$Q(x,t) = \int_0^t \phi(t-t') \int_0^\infty \int_0^\infty \gamma(t';\tau,\beta) g(\tau,\beta;x) d\tau d\beta dt' \qquad (3\text{-}3)$$

3.3 Numerical model

Numerical Monte-Carlo simulations are performed for generating τ-β simulation data. In Tasks 6A and 6B, the simulation data from the evaluation of the STT-1 test in TRUE-1 are used, and an approximate linear τ-β relationship inferred from the simulation data in TRUE-1 is used in the modelling of the breakthrough curves (BTCs)

In Task 6B2, Monte-Carlo simulations are performed for the specified configuration and boundary conditions (Figure 2-2) to produce simulation data of τ and β. The simulation data are then used directly in the modelling of the BTCs, i.e., no deterministic relationship between τ and β is assumed for Task 6B2.

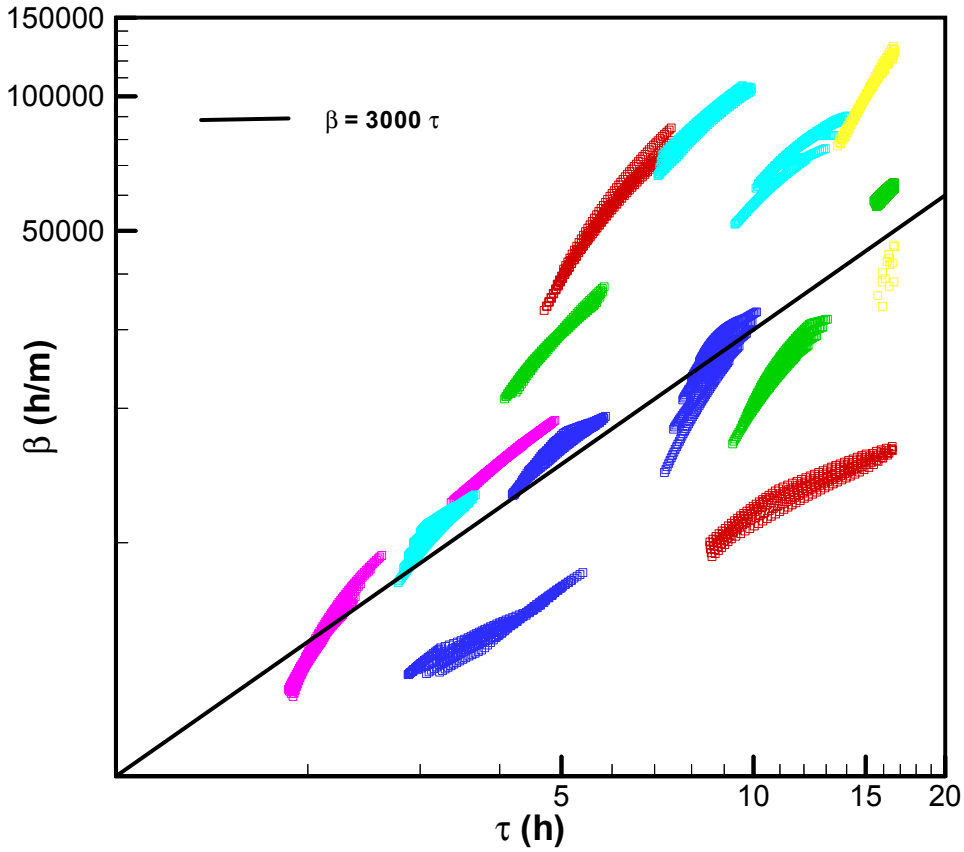

Figure 3-1. *The τ-β simulation data from the STT-1 test in the TRUE-1 program, plotted for some representative realisations. Each set of the lumped symbols represents the τ-β simulation data of 100 particles from one realisation. The straight line is the fitting line of β = 3000 τ.*

Tasks 6A and 6B

A linear β and τ relation, $\beta = 3000\tau$, inferred from the TRUE-1 program (Cvetkovic et al., 2000) is used for both Task 6A and Task 6B modelling. In Figure 3-1, the values of β and τ from the Monte-Carlo simulations in the TRUE-1 evaluation results (Cvetkovic et al., 2000) are plotted for some representative realisations. Each set of the lumped symbols in Figure 3-1 represents τ and β simulation data of 100 particles for one realisation. The solid line is the linear relation, $\beta = 3000\tau$, which represents approximately the average over the realisations. This linear relation $\beta = 3000\tau$ is used to calculate the BTCs of the tracers for Tasks 6A and 6B.

Task 6B2

In Task 6B2, Monte-Carlo simulations are performed to obtain simulated β and τ data. 21 particles are injected in each realisation. The averages over the 21 values for each realisation, $\overline{\beta}$ and $\overline{\tau}$, are calculated.

The flow equations are solved numerically for a randomly distributed fracture aperture field. The aperture fields are assumed to be lognormally distributed with an exponential correlation structure, i.e.,

$$b(\mathbf{x}) = b_G e^{Y(\mathbf{x})}$$

$$C_Y(r) = \sigma_Y^2 e^{-r/I_Y}$$

where r is the separation distance, b_G is the geometric mean, Y is a normally distributed random space function (RSF) with mean of zero and standard deviation of σ_Y, and I_Y is the (isotropic) integral scale of Y. It should be noted that b is the half aperture. A random generator HYDROGEN developed by Bellin and Rubin (1996) is used to generate the random aperture fields. 1000 realisations are generated.

The fracture plane with a size of 20×20 m^2 is discretized into 100×100 square elements with five elements per integral scale. Each element is assigned an aperture value randomly. In this modelling, σ_Y^2 is chosen to be 0.3 which is consistent with the TRUE-1 evaluation (Cvetkovic et al., 2000), the integral scale is 1 m. According to the task specification, a mean transmissivity of $T = 10^{-7}$ m^2/s is used in the modelling. Doe's law is assumed to be applicable locally (e.g., Outters and Shuttle, 2000), i.e.,

$$T = 4(2b)^2$$

where T is the transmissivity (m^2/s) and 2b is width of the aperture (m). When $\langle T \rangle = 10^{-7}$ m^2/s, $2b_G$ is computed from Doe's law as 0.14 mm.

As the random aperture fields are generated, the head fields are obtained using a standard, commercially available software (McDonald and Harbaugh, 1988). A constant head is assumed at the boundaries x = 0 and x = 20 m with a hydraulic gradient of 0.1%, whereas no flow condition is assumed at y = 0 and y = 20 m. The flow fields are then obtained using Darcy's law with Doe's law applicable locally.

When the flow fields are obtained, 21 particles are spaced evenly on a line section at x = 5.0 m, y = 9 to 11 m for particle tracking in each realisation. The τ and β values are recorded for these particles at the control line x = 15 m in each realisation. Figure 3-2 shows the scattergram for the mean values $\overline{\tau}$ and $\overline{\beta}$ of each realisation. These simulated $\overline{\tau}, \overline{\beta}$ values are used directly to obtain the breakthrough curves for each tracer in Task 6B2.

For the i*th* realisation, the breakthrough for pulse injection is calculated by

$$\gamma_i(t;\tau_i,\beta_i) = \frac{H(t-\tau_i-\beta_i K_a)\beta_i\kappa}{2\sqrt{\pi}(t-\tau_i-\beta_i K_a)^{3/2}} \exp\left[\frac{-\beta_i{}^2\kappa^2}{4(t-\tau_i\beta_i-K_a)}\right] \tag{3-4}$$

and for continuous injection of $\phi(t)$, it is calculated by

$$Q(t) = \int \phi(t-t')dt' \frac{1}{N}\sum_{i=1}^{N}\gamma_i(t';\tau_i,\beta_i) \tag{3-5}$$

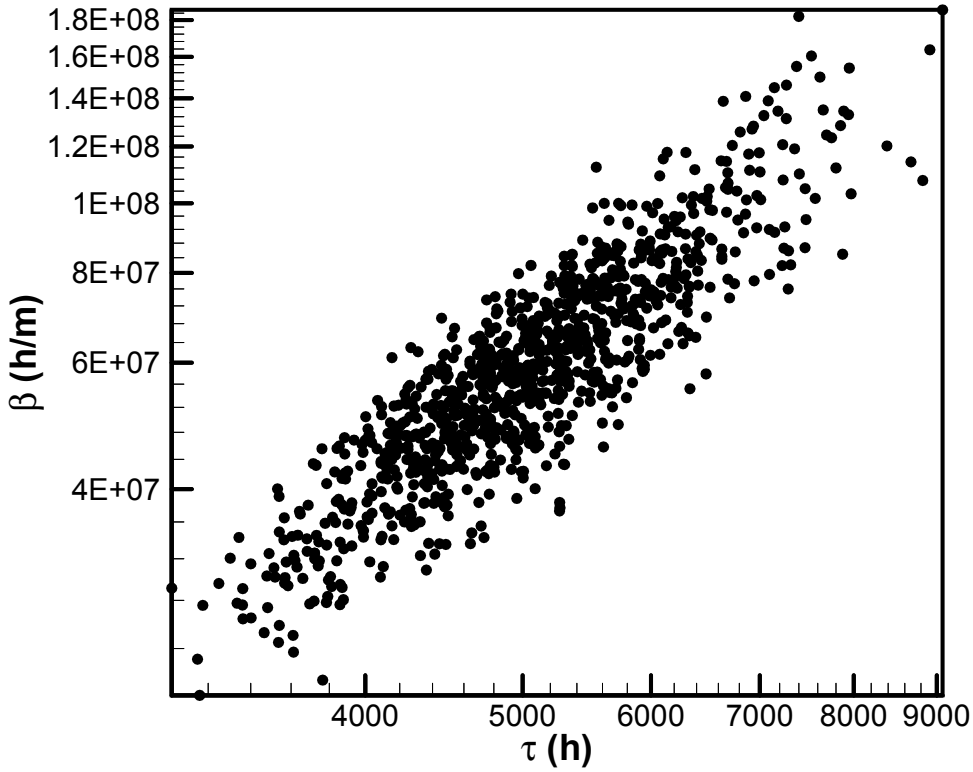

Figure 3-2. *Simulation data of $\overline{\tau}, \overline{\beta}$ for Task 6B2, one point from each realisation. The simulation data of τ and β shown in Figure 3-2 are used to calculate BTCs of tracers in Task6B2.*

3.4 Parameters

The most possible values of porosity, diffusion and sorption coefficients based on the TRUE-1 evaluation (Cvetkovic et al., 2000) are used in Tasks 6A and 6B.

The flow rate of injection shown in Table 3-1 was calculated from the dilution of the conservative tracer Uranine (Andersson et al., 1999). The flow rate is used to convert the provided concentration C (M/L^3) into flux Q (M/T).

Table 3-1. Injection flow rate calculated from the dilution of Uranine for STT-1b.

Elapsed time (h)	Flow rate (ml/h)
0-4	41.9
4-20	50
20-151	58.1

Below, we give the parameters used in the modelling.

Task 6A

- Surface sorption coefficient K_a: the MIDS value (Sr-85) (Byegård et al., 1998) and the data for additional tracers (Co-58, Tc-99m and Am-241) provided by Tasks 6A and 6B modeling task specification (Selroos and Elert, 2001) are used.

- Porosity: $\theta = 0.02$ based on the lower end of the TRUE-1 evaluation values (θ = 0.02-0,024) (Cvetkovic et al., 2000), which can be viewed as the best possible estimate. The porosity of 2% is also consistent with the statement in Tasks 6A and 6B Specification, i.e., for the short time period, the tracer retention occurs in the rock mass immediately adjacent to the fractures, most likely in fault gouge and adjacent cataclasite. In cataclasite, the porosity is 1.3%, and in fault gouge, the porosity is 10-20% (Selroos and Elert, 2001).

- Sorption coefficient K_d: the values used for different tracers are based on the batch data (fraction 1-2 mm) (Byegård et al., 1998), which are about 10 times of the MIDS value. It is implied in the TRUE-1 evaluation that K_d values were larger than the MIDS values, but were still consistent with the data of the batch test of fraction 1-2 mm. In the modelling, K_d values are chosen to be 10 times of the MIDS values or the values specified in Task Specification. The values for K_a (the surface sorption coefficient) are chosen to be the same as the MIDS values since K_a has relatively less effect on retention.

- The empirical Archie's law for the formation factor: $F = \theta^m$, where m = 1.2 is used. In the TRUE-1 evaluation, $F = \theta^{1.58}$. Here a power of m = 1.2 is used because it is believed that the micro fissures are more connected which yield lower values of m. The diffusivity D is then calculated by $D = \frac{FD_w}{\theta}$.

- The water residence time τ is assumed to be governed by an inverse-Gaussian distribution: The temporal moments from the TRUE-1 evaluation for the STT-1B test are used, i.e., the mean residence time is 5 h, and the variance is 1.5 h^2. The β parameter is assumed to have a linear relationship with τ, i.e., $\beta = 3000\tau$.

Task 6B

- Two sets of modelling calculations are conducted for two different porosity values. In the first set, the porosity is the same as that in Task 6A, i.e., $\theta = 0.02$. In the second set, $\theta = 0.01$. The reason for taking a lower porosity is that, as the time span becomes larger, there will be longer time for the tracer to diffuse more deeply into the rock matrix, where the porosity is smaller than that on the fracture surface.

- The same values of K_d and the power in Archie's law are used for Task 6B as for Task 6A.

- The water residence time τ is assumed to have an inverse-Gaussian distribution. Temporal moments are chosen based on simple reasoning of scaling. If the flow rate is 1000 time lower, then the mean travel time will be 1000 time longer. Therefore for Task 6B, a mean residence time of 5000 h is used. The variance is chosen so that the coefficient of variation is the same as that in Task 6A. The variance is therefore 1.5×10^6 h^2. The β parameter is still assumed to have a linear relationship with τ, i.e., $\beta = 3000\tau$.

Table 3-2 summarises the parameters used in the modelling of Tasks 6A and 6B.

Table 3-2. Summary of sorption and diffusion parameters used in Task 6A and 6B modelling

Tracer	Matrix sorption coefficient Kd (m^3/kg)		Surface sorption coefficient Ka (m)		Effective matrix diffusivity De×10^8 (m^2/h)		
	Task 6a	Task 6b	Task 6a	Task 6b	Task 6a	Task 6b	
					$\theta = 0.02$	$\theta = 0.02$	$\theta = 0.01$
I-131	0	0	0	0	5.4	5.4	2.4
Sr-85	4.7×10^{-5}	4.7×10^{-5}	8.0×10^{-6}	8.0×10^{-6}	2.6	2.6	1.1
Co-58	0.008	0.008	0.008	0.008	1.9	1.9	0.84
Tc-99m	2.0	2.0	0.2	0.2	2.6	2.6	1.1
Am-241	5.0	5.0	0.5	0.5	2.6	2.6	1.1

Task 6B2

- Two sets of modelling calculations are performed. The first set uses the MIDS data (Byegård et al., 1998) with a porosity of 0.004, and a density of the rock matrix of 2700 kg/m^3. The second set uses the most possible parameters from the TRUE-1 evaluation (the same as in Tasks 6A and 6B), i.e., the porosity $\theta = 0.02$, the K_d values are chosen to be 10 times the MIDS values or the values given in the Task Specification. The K_a values are the same as the MIDS values.

- We use Archie's law $F = \theta^{1.4}$ for both sets of modelling calculations. The diffussivity is calculated by $D = FD_w / \theta$

- The simulated τ, β values are used directly to calculate BTCs (Eq. (3-1) and Eq. (3-2)) for both sets of modelling calculations.

The moments of the τ and β data are shown in Table 3-3.

Table 3-3. First and second moments of the simulated τ and β data for Task 6B2.

$<\tau>$ (h)	σ_τ^2 (h^2)	$<\beta>$ (h/m)	σ_β^2 (h^2/m^2)
5113	9.16×10^5	6.2×10^7	5.35×10^{14}

Parameter set 1 (MIDS)

Porosity $\theta = 0.004$, density ρ=2700 kg/m^3, and

$$\kappa = \theta\sqrt{D(1 + K_d\rho/\theta)}$$

Parameter set 2 (as in the TRUE-1 evaluation)

$\theta = 0.02$, $F = \theta^{1.4}$, and $D = FD_w / \theta$

Table 3-4 lists the parameters used in the Task 6B2 modelling.

Table 3-4. Summary of sorption and diffusion parameters used in Task 6B2 modelling

Tracer	**Matrix sorption coefficient K_d (m^3/kg)**		**Surface sorption coefficient K_a (m)**	**Effective matrix diffusivity $D_e\times10^{10}$ (m^2/h)**	
	θ =0.004	θ = 0.02		θ =0.004	θ = 0.02
I-131	0	0	0	3.0	260
Sr-85	4.7×10^{-6}	4.7×10^{-5}	8×10^{-6}	1.4	120
Co-58	0.0008	0.008	0.008	1.0	88
Tc-99m	0.2	2.0	0.2	1.4	120
Am-241	0.5	5.0	0.5	1.4	120

3.5 Model calibration and development

Tasks 6A and 6B

The most possible estimates of sorption and diffusion parameters calibrated from the TRUE-1 evaluation are used here for tracers Sr-85 and Co-58. The porosity $\theta = 0.02$ used is consistent with the evaluation of TRUE-1. However the Archie's law is assumed to be $F = \theta^{1.2}$ where the power 1.2 is lower than the power 1.58 used in the TRUE-1 evaluation. The reason for this is explained in the previous section. The β and τ is assumed to have a linear relationship $\beta = 3000\tau$ in the Tasks 6A and 6B modelling which is consistent with the relationship obtained in the TRUE-1 evaluation. The best possible K_d values obtained from the TRUE-1 evaluation are about 10 times of the MIDS values. We therefore assume K_d values to be 10 times of the MIDS values or the values provided by Task Specification for consistency with the TRUE-1 evaluation.

Task 6B2

In Tasks 6A and 6B, the linear τ-β relationship is assumed. By assuming the linear relationship, the full variability of β parameter is neglected. In Task 6B2, the simulated β and τ data from Monte-Carlo simulations are used directly to compute BTCs, the τ variability and β variability are both accounted for independently.

4 Results - Performance measures

4.1 Task 6A

4.1.1 Drawdown in injection and pumping borehole

Not available.

4.1.2 Breakthrough time history for the tracers

Figure 4-1 shows the BTCs for the experimental injection for Task 6A. The black line is the BTC for tracer I-131, the red line for Sr-85, the green line for Co-58, and the blue line for Tc-99 m and the purple line for Am-241. This colour representation of the tracers will also be used in other figures throughout this report. The BTCs in Figure 4-1 could be roughly divided into three groups: the group for the conservative to weakly sorbing tracers (I-131 and Sr-85), the group for the moderately sorbing tracer Co-58, and the group for the strongly sorbing tracers Tc-99m and Am-241. The BTC for the conservative tracer I -131 is close to the BTC for the weakly sorbing tracer Sr-85. This result is consistent with that in the TRUE-1 evaluation. The BTC for Co-58 clearly shows stronger retention than those of I-131 and Sr-85 due to its stronger sorption and larger diffusion. The BTCs for Tc-99m and Am-241 show an even stronger retention while Am-241 has the strongest retention among the tracers studied in this work.

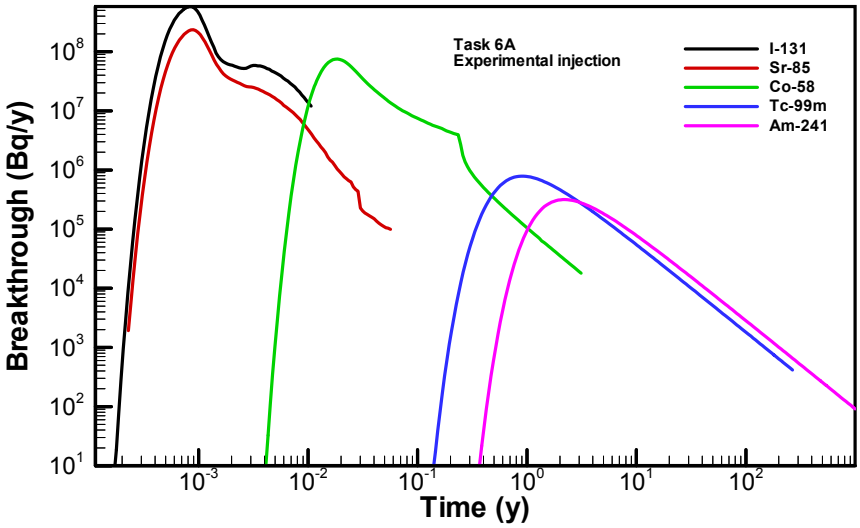

Figure 4-1. *Breakthrough curves for measured injection curves for Task 6A.*

Figure 4-2 shows the BTCs for Dirac pulse injection for Task 6A. The BTCs are similar to the BTCs shown in Figure 4-1 for the experimental injection.

Table 4-1 summarises the breakthrough times for 5%, 50% and 95% mass recovery. The masses of the conservative tracer I-131 and the weakly sorbing tracer are recovered most quickly. 95% of their injected masses are recovered within about 1.5×10^{-2} year (130 hours). For the moderately sorbing tracer Co-58 it takes longer time to recover 95% of the injected mass (0.7 year or 6100 hours). While for the strongest sorbing tracers Tc-99m and Am-241, it takes hundreds of years to recover the 95% injected mass.

Table 4-1. Breakthrough times for recovery of 5, 50 and 95% of the injected mass for Task 6A (years).

Tracer	T_5 (y)	T_{50} (y)	T_{95} (y)
I-131	5.9×10^{-4}	1.9×10^{-3}	1.5×10^{-2}
Sr-85	6.3×10^{-4}	1.6×10^{-3}	1.5×10^{-2}
Co-58	1.4×10^{-2}	5.0×10^{-2}	0.7
Tc-99m	0.7	4.0	217
Am-241	1.7	10.0	537

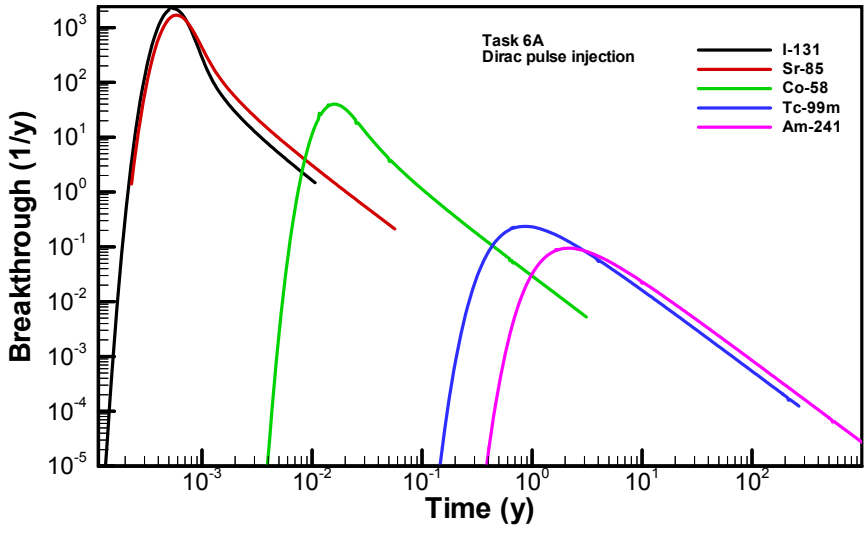

Figure 4-2. *Breakthrough curves for Dirac pulse injection for Task 6A.*

Table 4-2 lists the times for 5%, 50% and 95% mass recovery for Dirac pulse injection for Task 6A. These times are quite close to the respective times for the experimental injection in Table 4-1.

Table 4-2. Breakthrough times for recovery of 5, 50 and 95% of the Dirac pulse injection.

Tracer	T_5 (y)	T_{50} (y)	T_{95} (y)
I-131	3.9×10^{-4}	6.1×10^{-4}	2.0×10^{-3}
Sr-85	4.1×10^{-4}	7.1×10^{-4}	6.4×10^{-3}
Co-58	1.2×10^{-2}	2.5×10^{-2}	0.6
Tc-99m	0.7	4.0	217
Am-241	1.6	10.0	537

4.1.3 Maximum release rate

The maximum release rates are shown in Table 4-3 for the experimental injection in Task 6A. The conservative tracer I-131 has the highest maximum release rate. The Sr-85 has the rate in the same order of magnitude as that of I-131. Co-58 has the rate two orders of magnitude lower. While Tc-99m and Am-241 have the rates one more order of magnitude lower.

Table 4-3. Maximum release rate using measured injection curves for Task 6A.

Tracer	Max rate (Bq/y)
I-131	5.8e+8
Sr-85	2.4e+8
Co-58	7.5e+6
Tc-99m	7.9e+5
Am-241	3.2e+5

The maximum release rates for Dirac pulse injection are shown in Table 4-4 for Task 6A, which show similar trend as those in Table 4-3.

Table 4-4. Maximum release rate using Dirac pulse injection for Task 6A.

Tracer	Max rate (1/y)
I-131	2396
Sr-85	1687
Co-58	40.1
Tc-99m	0.24
Am-241	9.4e-2

4.2 Task 6B

4.2.1 Breakthrough time history for the tracers

The BTCs for a constant injection of 1MBq/y for Task 6B are shown in Figure 4-3, the BTCs for Dirac pulse injection in Figure 4-4. Two BTCs are presented for each tracer. The solid lines are for the case when porosity $\theta = 0.01$, and the dashed lines are for $\theta = 0.02$. Clearly the larger the porosity is, the stronger the retention. The tracers can also be divided into three groups as has been done in Task 6A.

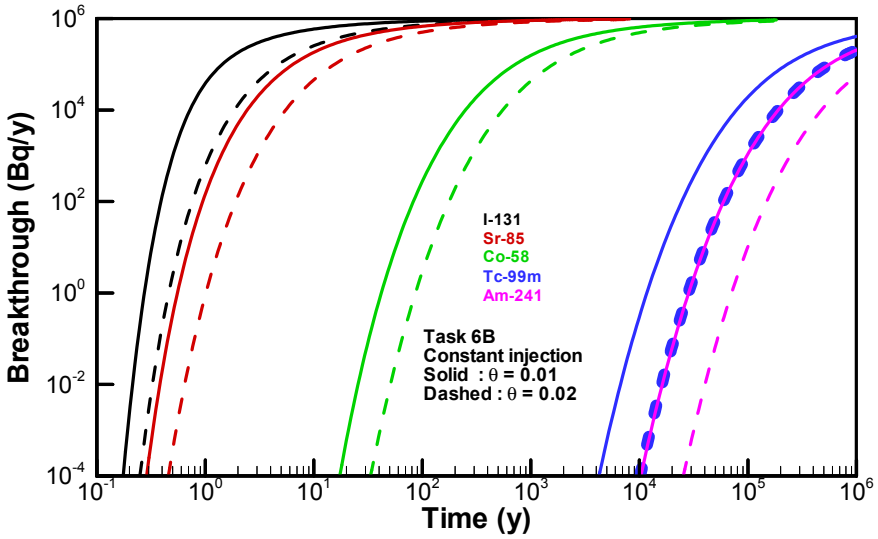

Figure 4-3. *Breakthrough curves for constant injection rate of 1MBq/year for Task 6B.*

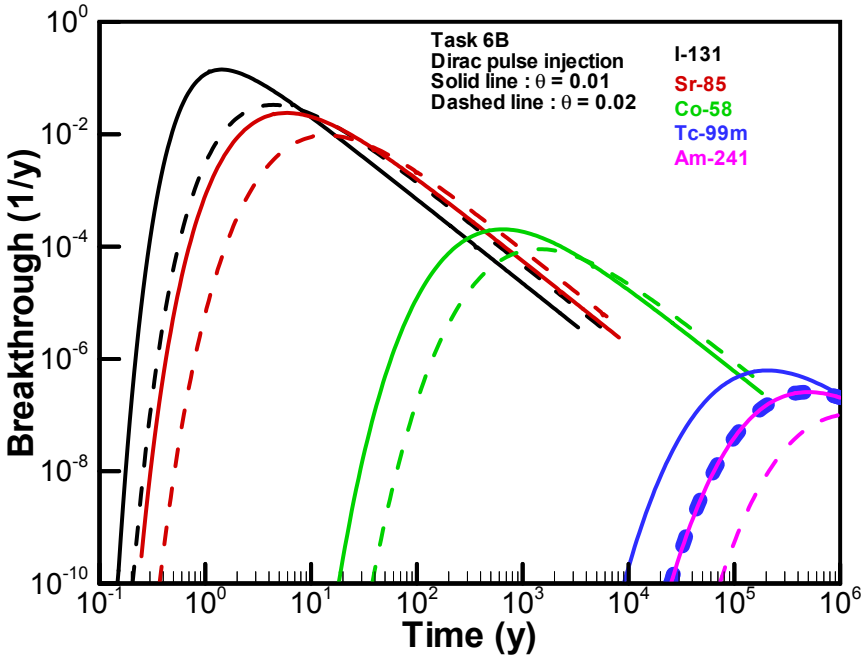

Figure 4-4. *Breakthrough curves for Dirac pulse injection for Task 6B.*

Table 4-5 shows the times for 5%, 50% and 95% mass recovery for Dirac pulse injection in Task 6B for both θ = 0.01 and θ = 0.02. The retention times for the different tracers have the same trend as in Task 6A, but several orders of magnitude longer. The masses of the conservative tracer I-131 and the weakly sorbing tracer are recovered most quickly. 95% of their injected masses are recovered within hundreds of years (compared to 0.002 years in Task 6A for Dirac pulse injection). For the moderately sorbing tracer Co-58 it takes thousands of years (e.g., more than 4000 years when θ = 0.01) to recover 50% of the injected mass (compared to 0.025 year in Task 6A for Dirac pulse injection). While for the strongest sorbing tracers Tc-99m and Am-241 it takes millions of years to recover 50% of the injected mass.

Table 4-5. Breakthrough times for recovery of 5, 50 and 95% of the Dirac pulse injection for Task 6B.

Tracer	T_5 (y)		T_{50} (y)		T_{95} (y)	
	θ = 0.01	θ = 0.02	θ = 0.01	θ = 0.02	θ = 0.01	θ = 0.02
I-131	1.1	3.2	6.7	26.4	376	947
Sr-85	4.4	10.4	38.8	98.2	2283	5708
Co-58	479	1073	4566	10388	-	-
Tc-99m	1.5e+5	3.8e+5	1.5e+6	-	-	-
Am-241	3.8e+5	9.4e+5	-	-	-	-

4.2.2 Maximum release rate

The maximum release rates for Dirac pulse injection in Task 6B are shown in Table 4-6. Compared to Task 6A, the maximum release rates are much lower in Task 6B.

Table 4-6. Maximum release rate using Dirac pulse injection for Task 6B.

Tracer	Max rate (1/y)	
	θ =0.01	θ =0.02
I-131	0.14	3.3e-2
Sr-85	2.4e-2	9.6e-3
Co-58	2.0e-4	9.0e-5
Tc-99m	6.2e-7	2.6e-7
Am-241	2.6e-7	-

4.3 Task 6B2

4.3.1 Breakthrough time history for the tracers

The BTCs for a constant injection of 1 MBq/y are shown in Figure 4-5 for Task 6B2, and for Dirac pulse injection in Figure 4-6. The solid lines are for porosity θ = 0.004 (the MIDS value), and the dashed lines are for θ = 0.02. Large deviation between the BTCs for these two porosities can be observed. These two BTCs for each tracer can be viewed as two bounds of the modelling results.

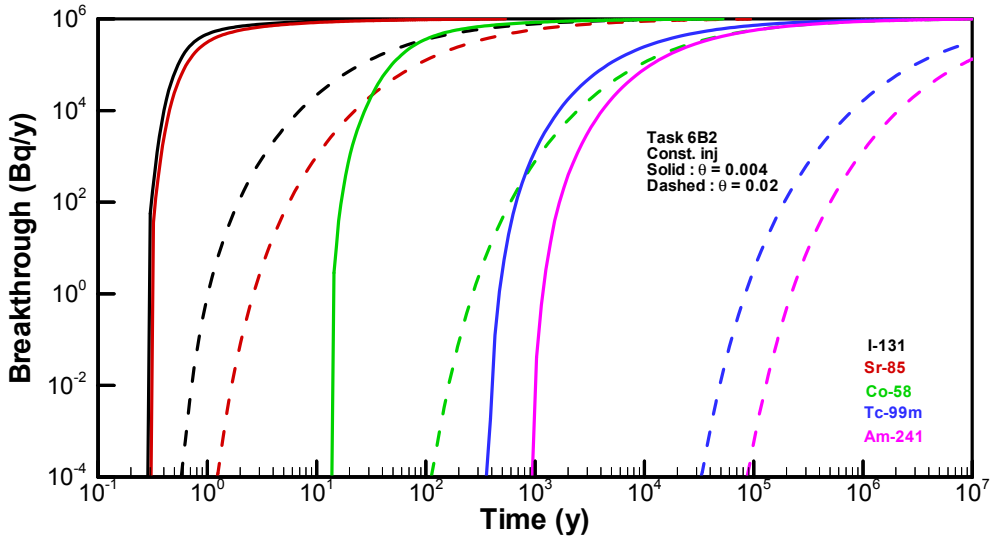

Figure 4-5. *Breakthrough curves for constant injection rate of 1MBq/year for Task6B2.*

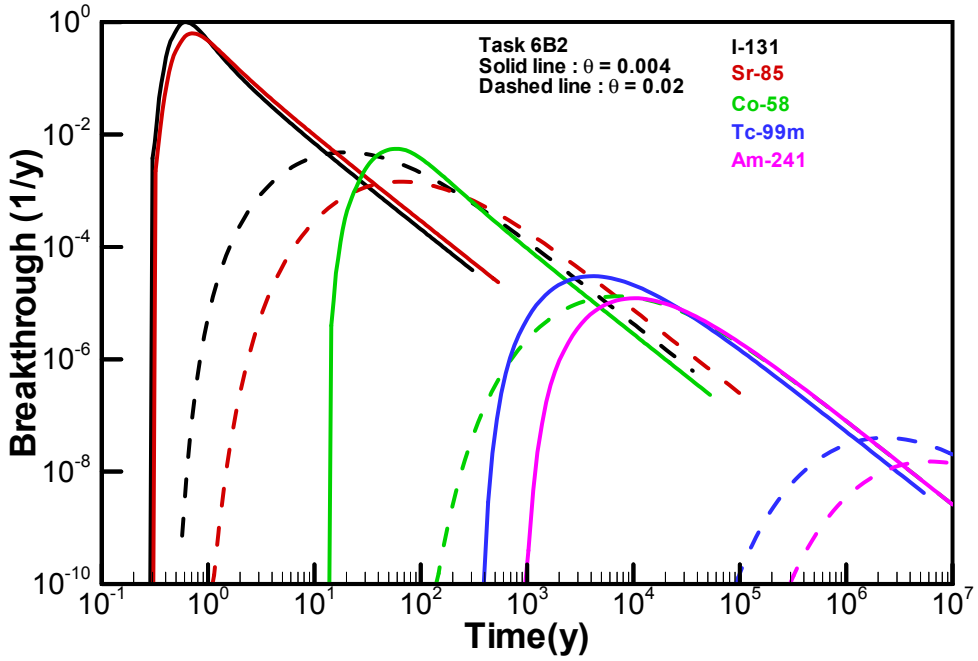

Figure 4-6. *Breakthrough curves for Dirac pulse injection for Task 6B2.*

The times for 5%, 50% and 95% of mass recovery are listed in Table 4-7. For the two values of porosity, the recovery times are quite different. It takes much shorter time to recover the same amounts of mass when the porosity is low. The recovery times for θ = 0.02 in Task 6B2 are within the same order of magnitude as in Task 6B when the porosity is the same. For detailed comparison of results between Tasks 6B and 6B2, see the next chapter.

4.3.2 Maximum release rate

The maximum release rates are shown in Table 4-8 for Dirac pulse injection for Task 6B2. The same tracer has a much higher maximum release rate when the porosity is low.

Table 4-7. Breakthrough times for recovery of 5, 50 and 95% of the Dirac pulse injection for Task 6B2.

Tracer	T_5 (y)		T_{50} (y)		T_{95} (y)	
	θ=0.004	θ = 0.02	θ=0.004	θ = 0.02	θ=0.004	θ = 0.02
I-131	0.5	16	1.0	1.9e+2	18	7.7e+3
Sr-85	0.55	51	1.5	6.4e+2	36	2.5e+4
Co-58	38	5.6e+3	140	7.2e+4	3300	2.8e+6
Tc-99m	3.1e+3	1.8e+6	3.0e+4	2.3e+7	1.1e+6	9e+8
Am-241	7.7e+3	4.9e+6	7.5e+4	6.1e+7	2.8e+6	2.5e+9

Table 4-8. Maximum release rate using Dirac pulse injection for Task 6B2.

Tracer	Max rate (1/y)	
	θ=0.004	θ =0.02
I-131	1.0	5e-3
Sr-85	0.6	1.5e-3
Co-58	5.6e-3	1.3e-5
Tc-99m	3e-5	4e-8
Am-241	1.2e-5	1.5e-8

5 Discussions

5.1.1 Conceptual issues

Figure 5-1 shows the comparison of the modelled BTCs between Tasks 6B and 6B2 using the same porosity $\theta = 0.02$ and the same sorption coefficient. The powers in the Archie's law used in the two tasks are slightly different (1.2 and 1.4 respectively).

The differences between the BTCs are obvious in Figure 5-1. The BTCs of Task 6B2 show stronger retention than those in Task 6B. In Task 6B, the water residence time τ is assumed to be an inverse-Gaussian distribution, and the parameter β is assumed to have a deterministic linear relation with τ, i.e., $\beta = 3000\tau$. The variability of β is neglected. In Task 6B2, both simulated τ and β data are used directly in calculating the BTCs, therefore the variability of β is accounted for independently of τ.

The means of τ used in Task 6B and 6B2 are both about 5000 h. In Eq. 3-1, the BTCs are determined by two groups of parameters, βK_a and $\beta\kappa$. In the modelling for all the three subtasks, the same K_a values (the MIDS values) are used for the same tracer. Strong influences of K_a on the modelled results are not expected. The differences between the modelled BTCs between Tasks 6B and 6B2 in Figure 5-1 could therefore be dominantly influenced by the parameter β through the parameter groups, βK_a and $\beta\kappa$.

In the following, we will examine the influences of β and κ separately. It then follows the discussions of the influences of the product of these two parameters.

Table 5-1 lists the means of β. The values of β used in Task 6B2 are about 4 times of those used in Task 6B.

Table 5-1. Means of β. For Task 6B, the mean value of β is obtained through $\beta = 3000\tau$. For Task 6B2, the ensemble mean of β is shown.

	$<\beta>$ (h/m)
Task 6B	1.5×10^7
Task 6B2	6.2×10^7

Table 5-2 lists the κ values used in obtaining the BTCs in Figure 5-1. The κ values for Task 6B2 are about 30% lower compared with those for Task 6B. This implies that in Task 6B2 the retention due to diffusion/sorption in the rock matrix is weaker than in Task 6B. In Figure 5-1, however, it shows that the tracers have stronger retention in Task 6B2 than in Task 6B. The reason is believed to be that the products of β with κ and K_a, i.e., the parameter groups $\beta\kappa$ and βK_a, determine the retention of the tracers. In Task 6B2, $<\beta>$ is about four times of that in Task 6B. Even though κ is smaller in Task 6B2, the overall retention of the tracers is determined by the parameter group $\beta\kappa$ and is still larger in Task 6B2 compared with that in Task 6B. A larger β also implies a larger product βK_a.

Table 5-2. Values of the parameter κ used in calculating BTCs in Figure 5-1.

Tracer	κ (m/h$^{1/2}$)		<β>κ (h$^{1/2}$)	
	Task 6B	Task 6B2	Task 6B	Task 6B2
I-131	3.3×10^{-5}	2.3×10^{-5}	5×10^{2}	14.3×10^{2}
Sr-85	6.2×10^{-5}	4.2×10^{-5}	9.3×10^{2}	26.0×10^{2}
Co-58	6.4×10^{-4}	4.4×10^{-4}	9.6×10^{3}	27.3×10^{3}
Tc-99m	1.2×10^{-2}	8.0×10^{-3}	1.8×10^{5}	5.0×10^{5}
Am-241	1.9×10^{-2}	1.3×10^{-2}	2.9×10^{5}	8.1×10^{5}

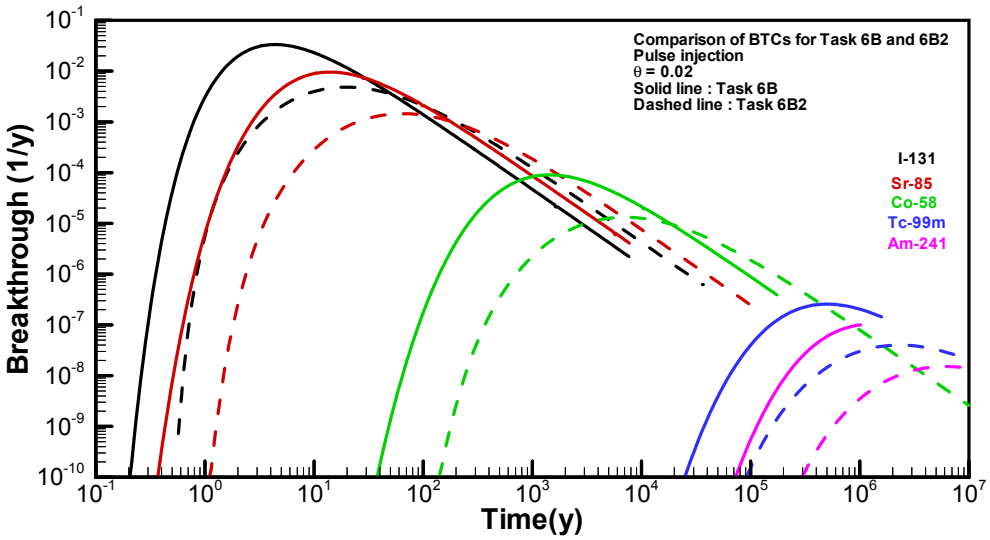

Figure 5-1. *Comparison of the BTCs for Tasks 6B and 6B2 using $\theta = 0.02$.*

5.1.2 Lessons learned

The LaSAR approach seems suitable both for evaluating the site characterisation results and in providing reasonable estimates for the performance assessment modelling.

In Task 6A, the BTCs and the times for 5, 50 and 95% mass recovery are comparable for both the experimental injection and the Dirac pulse injection. This could imply that, as long as the injection duration is not so long, the injection history has relatively small influences on the retention of the tracers.

In Task 6B, the influences of porosity on tracer retention are apparent. For Dirac injection, the ratios between the respective mass recovery times for the two porosities are always larger than the ratio of the porosity itself (which is 2). This indicates that the influences of the porosity is non-linear and are larger for larger porosities.

The modelling results of Tasks 6B and 6B2 show that the parameter β has a strong influence on retention and transport, and therefore on the breakthrough curves of the tracers.

In the Task 6B2 simulations, the values of τ and β were obtained from direct Monte Carlo simulations and used to calculate the BTCs assuming Doe's law. In Tasks 6A and 6B, the linear τ-β relationship obtained from TRUE-1 evaluations has been used to calculate the BTCs, assuming cubic law. The first and second moments of water residence time τ used in Task 6B are consistent with the simulation results of Task 6B2 in this study. However, it is difficult to directly compare the results between Task 6B and Task 6B2 since they have different boundary conditions. The influence of Doe's law can be assessed by sensitivity analysis as part of future work (e.g., in Task 6D modelling), by considering comparable boundary conditions. Similarly, the influence of the variance change of the transmissivity can be studied as part of future Tasks.

6 References

Andersson, P., Wass, E., Johansson, H., Skarnemark, G., and Skålberg, M., 1999. TRUE 1st stage tracer test programme. Tracer tests with sorbing tracers, STT-1b. Experimental description and preliminary evaluation. International progress report IPR-99-12, SKB.

Bellin, A. and Rubin, Y., 1996. HYDRO_GEN: A spatially distributed random field generator for correlated properties. Stoch. Hydrol. Hydraul. 10, 253-278.

Byegård, J., Johansson, M. and Tullborg, E-L., 1998. The interaction of sorbing and nonsorbing tracers with different Äspö rock types:Sorption and diffusion experiments in the laboratory scale. Technical Report TR-98-18, SKB.

Cvetkovic, V., Selroos, J.-O., and Cheng, H., 1999. Transport of reactive tracers in rock fractures. J. Fluid Mech., 378, 335-356.

Cvetkovic, V., Cheng, H., and Selroos, J.-O., 2000. Evaluation of Tracer Retention Understanding Experiments (first stage) at Äspö, International Cooperation Report, ICR-00-01, SKB.

Cvetkovic V., and Cheng, H., 2002. Evaluation of block scale tracer retention understanding experiments at Äspö HRL. Swedish Nuclear Fuel and Waste ManagementCompany (SKB). Äspö Hard Rock Laboratory. International Progress Report IPR-02-33.

Elert, M., and Selroos, J.-O., 2001. Task 6B2 modelling task specification. SKB.

McDonald, M. G. and Harbaugh, A. W., 1988. A modular three-dimensional finite-difference ground-water flow model. Techniques of Water-Resources Investigations of the United States Geological Survey, Book 6. Scientific Software Group, Washington, D.C.

Outters, N. and Shuttle, D., 2000. Sensitivity analysis of a discrete fracture network model for performance assessment of aberg. Report R-00-48, SKB.

Selroos, J.-O., and Elert, M., 2001. Task 6A & 6B modelling task specification. SKB.

Winberg, A., Andersson, P., Hermanson, J., Byegård, J., Cvetkovic, V., and Birgersson, L., 2000. Äspö Hard Rock Laboratory, Final report of the first stage of the tracer retention understanding experiments. Technical report TR-00-07, SKB.